# Stability of Jupiter Trojans investigated using frequency map analysis: the MATROS project

F. Marzari,[1]⋆ P. Tricarico[1] and H. Scholl[2]

[1]*Department of Physics, University of Padova, Via Marzolo 8, 35131 Padova, Italy*
[2]*Observatoire de la Côte d'Azur, BP 4229, 06304 Nice Cedex 4, France*

**ABSTRACT**

Using the frequency map analysis (FMA) method we investigate the stability properties of Trojan-type orbits in the proximity of the $L_4$ and $L_5$ Lagrangian points of Jupiter. This study is part of the MATROS project. The orbits of about $2 \times 10^4$ virtual Trojans with random initial conditions have been computed numerically and for each body the diffusion rate in frequency space has been determined by spectral analysis. The diffusion portraits show where stable orbits are located in the space of proper elements for different values of inclination. For low inclined orbits we reproduce the stability region outlined by Levison, Shoemaker & Shoemaker and, due to our fast sampling capability, we find additional resonant features in the libration amplitude versus proper eccentricity space. At higher inclinations, the stability region gradually shrinks and it disappears for inclinations of about $40°$. The maximal Lyapunov characteristic exponent is computed for a limited number of Trojan orbits in our sample and the predictions concerning the chaotic behaviour of each orbit are compared with those given by the FMA method. A good agreement is obtained and the value of the Lyapunov exponent may be used to tune the results of the FMA analysis. A synthetic secular theory for the proper frequencies of Jupiter Trojans is obtained by numerically fitting the outcome of the frequency map analysis.

**Key words:** celestial mechanics – minor planets, asteroids.

## 1 INTRODUCTION

The stability of Jupiter Trojans, a consistent group of asteroids orbiting about the $L_4$ and $L_5$ Lagrangian points of Jupiter, has been investigated by several authors using different models (see Marzari et al. 2003 for a review). This interest is motivated by the intrinsic complexity of the resonant motion of these bodies and by the difficulty of developing an analytic predictive theory able to outline their stability properties. The Trojan motion at the Lagrangian points of Jupiter can, in fact, be perturbed by additional dynamical mechanisms such as secular resonances with the fundamental frequencies of the Solar system, secondary secular resonances and three-body mean motion resonances related to the great inequality between Jupiter and Saturn. Even the overlapping of resonances close to the planet can contribute to the erosion of the volume in phase space where stable Trojan orbits can exist.

In this paper we adopt a numerical approach based on the frequency map analysis (FMA) method described in Laskar, Froeschlè & Celletti (1992), Laskar (1993a,b) and subsequently improved by Šidlichovský & Nesvorný (1997). The major advantage of this

method is to require short-term numerical integration of test Trojan orbits to outline the stability properties. It allows a rich sampling of the phase space without demanding a heavy CPU-time load. Our work extends that of Levison et al. (1997) since we consider different slices in inclination while the sample of Levison et al. (1997) was started in the same orbital plane of Jupiter. Moreover, taking full advantage of the power of the FMA method, we can describe in more detail the features of the stability regions by studying the dynamical properties of more than $2 \times 10^4$ virtual Trojans against the 270 analysed by Levison et al. Their results stand, however, as a reference for the long-term behaviour within the stability regions which we outline with the FMA method. For some significant cases we also compare the predictions of the FMA method with the estimated values of the maximal Lyapunov characteristic exponent. The comparison indicates that the two methods are in very good agreement, which supports the reliability of the FMA approach as an indicator of chaos.

The stability of Jupiter Trojans is described by their diffusion in a phase space defined by proper libration amplitude and proper eccentricity for fixed proper inclination. The resulting figures are called diffusion maps. It turns out that the stability regions decrease with increasing inclination. Multiplet structures that represent a mixture of regions with different dynamical lifetimes appear at low

⋆E-mail: marzari@pd.infn.it

inclinations. We discuss critically the various features found in the diffusion maps. In order to investigate the influence of Saturn, Uranus and Neptune on the stability of Jupiter Trojans, we integrated some cases in the Sun–Jupiter–Trojan model and compared the resulting diffusion maps with the full model including all outer planets.

Using the proper elements and proper frequencies estimated by the FMA method, we have built an 'empirical' secular theory for Jupiter Trojans. We fit the main frequencies, i.e. the circulation period of the perihelion longitude and of the node, and the libration frequency with polynomial expressions in the proper orbital elements as in Milani (1994). This synthetic theory may be used as reference for more sophisticated fully analytical theories (Beaugé & Roig 2001).

## 2 THE NUMERICAL INTEGRATION

We used the WHM integrator (Wisdom & Holman 1991) to perform all the numerical integrations which is part of the SWIFT software package (Levison & Duncan 1994). Each virtual Trojan orbit is computed over a time-span of 2.5 Myr within a six-body model including the four major outer planets Jupiter, Saturn, Uranus and Neptune. This time-span is long enough for the FMA method to determine with high precision the diffusion rate in the action space using the running window method. It also allows a good determination of the proper frequencies $g$ and $s$ of each orbit by analysing the non-singular variables $h$, $k$ and $p$, $q$. In parallel, we integrated the same initial conditions but for only $2 \times 10^5$ yr and with a short interval of time between two subsequent output sets in order to compute the libration frequency $f_L$. Additional simulations within the full three-body problem (Sun–Jupiter–asteroid) were also carried out for comparison with the six-body model results. The time series of the orbital elements are digitally filtered in order to remove all the short periods smaller than 100 yr (Carpino, Milani & Nobili 1987; Marzari, Tricarico & Scholl 2002b). In this way we attenuate the short-period terms related to the orbital period of Jupiter, Saturn and Uranus, and we do not affect the libration period of Trojan orbits, which are longer than 150 yr.

The computation of the initial orbital element list for the virtual Trojans is based on a preliminary short-term integration of random initial conditions lasting $10^5$ yr. The starting semimajor axis for each Trojan is selected within an interval ranging from 0.9 to $1.1a_J$, where $a_J$ is equal to the initial semimajor axis of the orbit of Jupiter; the eccentricity is chosen randomly between 0 and 0.25; all the orbital angles are selected at random between 0° and 360°. Five different sets of initial conditions are computed, each for a fixed value of inclination: 0°, 10°, 20°, 30° and 40°. This preliminary integration allows one to avoid computation over a long time-span of Trojan orbits, which would become unstable after a short period. At the end of this pre-integration only those orbits with a librating critical argument $\lambda - \lambda_J$ are included in the sample of virtual Trojans for the main integration, which covers 2.5 Myr. The preliminary integration takes about 20 h of CPU time to produce a list of 1000 Trojan orbits, while the main integration of 1000 orbits over 2.5 Myr takes about 4 d of CPU time on a pentium IV at 2 GHz. The size of the output files to be analysed with the FMA method is about 800 MB. For each slice of fixed initial inclination we compute about 5000 bodies with the exception of the cases at high inclination where the stability region is narrower and fewer bodies are necessary.

The initial orbital elements of the planets are taken from the JPL ephemeris and are referred to the invariable plane of the Solar system.

## 3 TOOLS FOR THE STABILITY ANALYSIS

### 3.1 The FMA method

The FMA technique was introduced by Laskar et al. (1992); Laskar (1993a,b). The basic idea behind this method is to analyse the evolution in time of one or more fundamental frequencies of a dynamical system from the outcome of a numerical integration. Measuring the diffusion rate of a frequency with the running windows method yields a measure of chaos. Being much faster than the Lyapunov exponent computation, the FMA method is better suited to estimating the size and shape of the chaotic zones of a dynamical system.

We briefly recall here the FMA theory and the numerical algorithm we have implemented to evaluate the frequencies and their variations. Given a quasi-periodic complex function $f(t)$, we can represent it as a Fourier expansion in the following form:

$$f(t) = \sum_{n=1}^{\infty} a_n e^{i(\nu_n t + \phi_n)}, \tag{1}$$

where $a_n$ are real amplitudes decreasing with $n$ while $\nu_n$ and $\phi_n$ are the corresponding frequencies and phases, respectively.

The FMA method consists in finding a set of $N$ peaks $\{a'_n, \nu'_n, \phi'_n\}$ so that the reconstructed signal $f'(t)$, given by

$$f'(t) = \sum_{k=1}^{N} a'_n e^{i(\nu'_n t + \phi'_n)} \tag{2}$$

approximates the original $f(t)$ up to a fixed accuracy. If the function $f(t)$ is the numerical solution of a dynamical system, we have the tabulated values of $f(t)$ at evenly spaced intervals of time d$t$ over a time-span $\Delta T$. We can compute with high precision the frequencies $\nu_n$ over a running window $[T_i, T_{i+1}]$ covering the interval $\Delta T$. The dispersion of the frequencies estimated by the standard deviation of $\nu_n$ calculated on the running windows measures the diffusion rate of the solution $f(t)$ in the action space.

A recursive algorithm to perform the frequency analysis of a signal is described in detail by Šidlichovský & Nesvorný (1997). High precision in the computation of each frequency is achieved by the use of Hanning windowing. Gramm–Schmidt orthogonalization enables one to efficiently subtract each peak step by step from the signal. Šidlichovský & Nesvorný (1997) even extend the original method by Laskar (labelled MFT in their paper), by applying linear corrections to the frequency of the peaks (FMFT, frequency modified Fourier transform). We implemented both the algorithms, but in the testing phase the MFT has proven to be more stable than the FMFT, especially when the function $f(t)$ is quite far from being quasi-periodic, i.e. in the case of fast diffusing orbits. For this reason we preferred the MFT version of the FMA for the analysis presented in this paper. The computer algorithm we have used is available as part of the ORSA framework at http://orsa.sourceforge.net.

To analyse the outcome of the integrations of Jupiter Trojan orbits using the FMA method, we concentrated on the non-singular variables $h$ and $k$, defined as $h = e \cos(\tilde{\omega})$ and $k = e \sin(\tilde{\omega})$. For each orbit we compute the proper frequency $g$ and its amplitude, the proper eccentricity $e_p$ (Milani 1993), over running windows of $2 \times 10^5$ yr over the 2.5 Myr of numerical integration. As a measure of the diffusion rate, we use the negative logarithm of the standard deviation $s_g$ of $g$ over the 24 windows: $\sigma = -\log_{10}(s_g/g)$. Typical values of $\sigma$ range from 5 for stable orbits down to 1 for highly chaotic orbits.

The variables $p$ and $q$ have also been analysed to derive the proper frequency $s$ and its amplitude, the sine of the proper inclination

$\sin(I_p)$. Since $s$ is smaller than $g$, we have used the full time-span of the integration (2.5 Myr) to estimate $s$ from the spectrum of $p$ and $q$. The quantities $e_p$ and $\sin(I_p)$ are also referred to as free eccentricity and free inclination, to distinguish them from the forced components.

When the FMA analysis is concluded, each orbit is labelled by the value of $e_p$ computed in the first window $[T_0, T_1]$ and adopted as the proper eccentricity of the orbit, by $\sin(I_p)$ computed over 2.5 Myr, and by the dispersion $\sigma$ of the proper frequency $g$. The libration amplitude $D$ is computed independently from the FMA method. Instead of following the recipe of Milani (1993, 1994) we have slightly modified his procedure in order to compute $D$ on a shorter time-scale. Some of the orbits in our sample are chaotic and the libration amplitude can change within some Myr. We need an algorithm, even if less sophisticated than that of Milani, allowing us to compute $D$ over a short time-span so that $D$ does not vary significantly for the chaotic nature of some of the orbits. We estimate the proper $D$ for each Trojan orbit as the mean of the maximum libration amplitude computed on running windows of $2 \times 10^4$ yr over the first $2 \times 10^5$ yr of our 2.5 Myr numerical integration. Taking into account that most of the short-term perturbations had already been removed by the digital filter that cuts all perturbations with periods of less than 100 yr, with our algorithm we indeed obtain a good estimate of the proper $D$. To check the accuracy of our procedure for computing proper $D$ values, we have compared our values for real Trojans with those determined by Milani (1993). The agreement was within 8 per cent for the smaller values of $D$ (notice that, by definition, our value of $D$ corresponds to twice that given by Milani) and steadily decreased to 2 per cent for larger libration amplitudes; in other words, the difference was always less than $1°$. Taking into account that there are also slight differences in the initial osculating orbital elements and in the integration methods, this appears to be a good match with Milani's estimates.

Our sample of fictitious Trojans include orbits with various diffusion rates and hence different degrees of chaotic behaviour. There are orbits that are stable over some Gyr and orbits that evolve on time-scales of some Myr. If by the term 'proper elements' we mean quantities related to possible constants of motion, then they are well defined only for stable orbits. In this paper we use the term in its broader sense, i.e. elements related to the proper frequencies of the motion. They are, in fact, used to label the initial position of an orbit in the action space and, for chaotic orbits, they are constant only over a limited interval of time. Our definition appears to be consistent in terms of continuity. Indeed, all the Trojan orbits in our sample appear to have some degree of chaotic evolution, even those with a lower diffusion rate. Consequently, proper elements can indeed change even for what we term stable orbits, possibly on time-scales longer than the age of the Solar system.

In principle, the best way to select the initial conditions would be to define slices in *proper* rather than in *initial* inclination. This would be very expensive and inefficient in terms of CPU time since it requires the integration of thousands of orbits and the application of the FMA to all of them to derive the proper inclination. Finally, we should group them around particular values in inclination, throwing away those orbits with intermediate values of $I_p$. However, the method of fixing the initial inclination is also viable since in our integrations the proper values $I_p$ are in most cases clustered within a band around the initial inclination $I_0 \pm 1°$. The orbits outside the bands, apart from the case with $I_0 = 0°$, have a value of $I_p$ lower than $I_0$. This is a dynamical effect: very often these orbits are located close to the location of a nodal secular resonance where the forced term is large and contributes significantly to $I_0$. This phenomenon
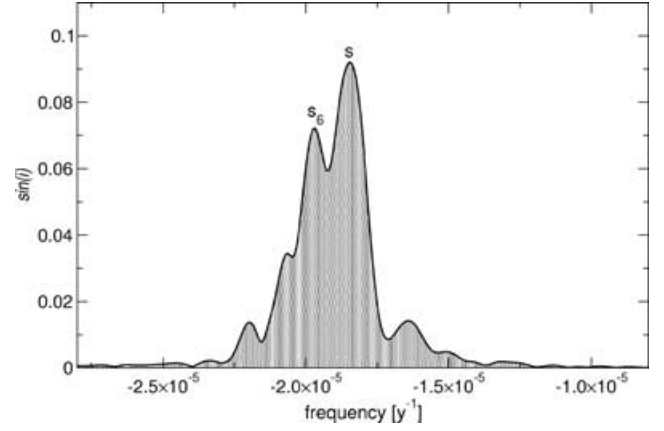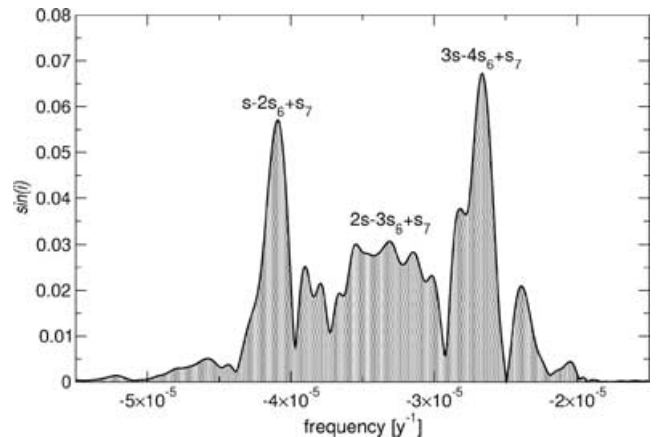


**Figure 1.** Spectrum of the $p, q$ variables for a body close to the $s_6$ secular resonance. The peak of the forced component is not negligible with respect to the proper one and, consequently, $I_p$ is lower than $I_0$.

is illustrated in Fig. 1 for a body with an initial inclination of $10°$ located close to the $s_6$ secular resonance. The forced peak is very close to the proper one and both of them contribute significantly to the initial $I_0$ value. The cases with $I_0 = 0°$ differs in the sense that $I_p$ will be larger than $I_0$ for those cases where $I_p$ is comparable to the forced term. In Fig. 3 (top plot, the case with $I_0 = 0°$) later, we notice that all the data with $I_p > 1°$, marked by a black dot, are located along the $s_6$ secular resonance.

In other cases, the difference between $I_p$ and $I_0$ is caused by the highly chaotic nature of the orbit. The diffusion is so fast that even the proper frequency $s$ changes over a short time-scale, causing a broadening of the peak in the spectrum of the $p, q$ variables. Consequently, the proper inclination is not well defined. There is nothing to be done for this since we need a time-span of at least 2.5 Myr to precisely retrieve the frequency $s$ in the spectrum while the orbit is chaotic on a shorter time-scale. An extreme example of this behaviour is shown in Fig. 2 where the proper frequency passes through different secular resonances.

What should we do with these orbits? Should we keep them in the sample labelled by the initial inclination $I_0$ or should we reject them? We decided to keep these orbits but when we draw the diffusion maps, we distinguish them with a different symbol.



**Figure 2.** Spectrum of the $p, q$ variables for a body on a highly chaotic orbit. The forced components of different secular resonances dominate while the proper component is spread over a range of frequencies.
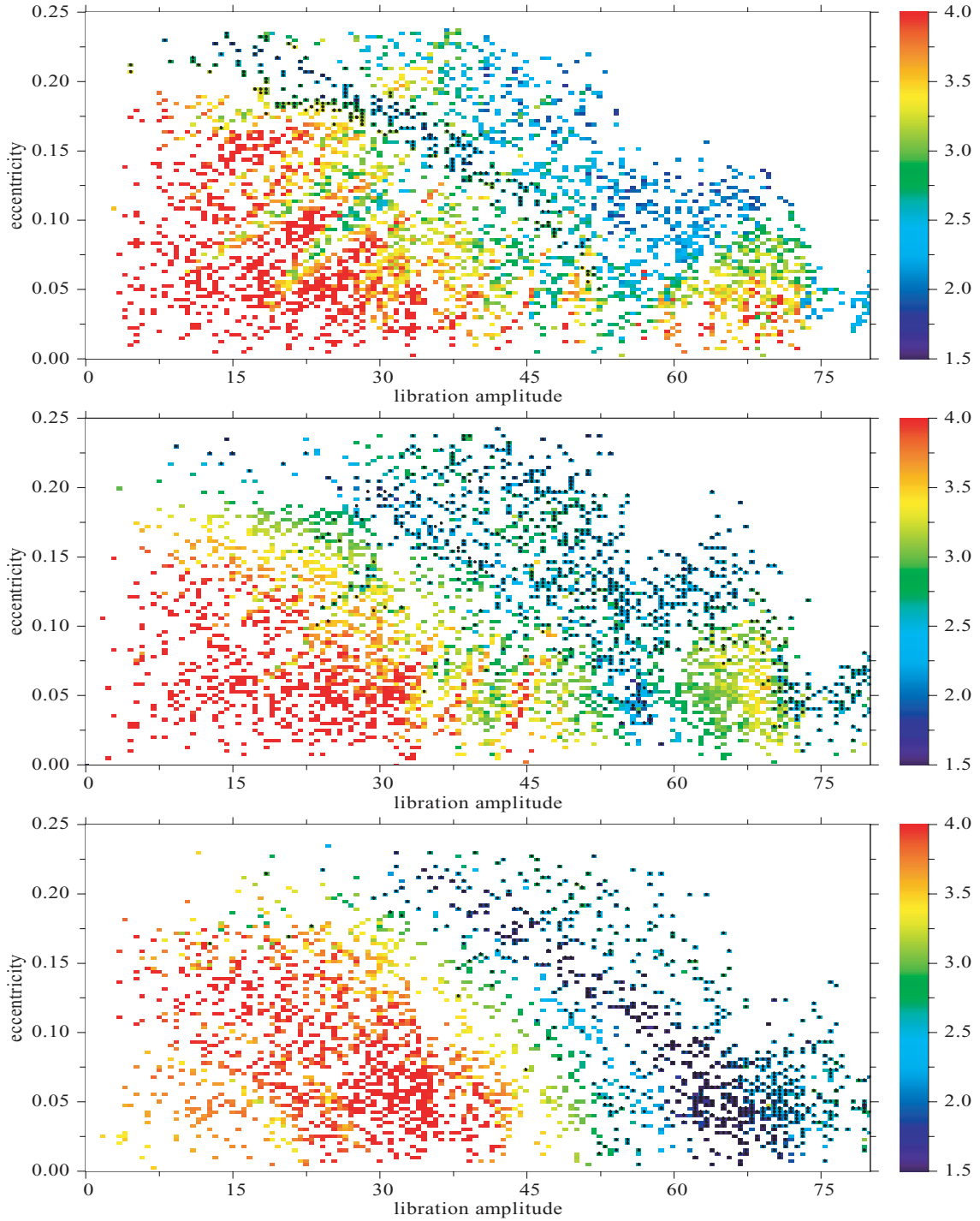
**Figure 3.** Diffusion portraits of Trojan orbits for different initial inclinations. The colour coding refers to different values of the diffusion coefficient $\sigma = -\log_{10}(s_g/g)$. From top to bottom, $I_0 = 0°, 10°, 20°$. The black dots mark those orbits with $I_p$ outside the band $I_0 \pm 1°$. Continued on next page: from top to bottom, $I_0 = 30°, 40°$. The last plot on the bottom shows orbits with $I_0 = 0°$ and fixed frequencies in $\tilde{\omega}$ with periods: $3465 \pm 8$, $3527 \pm 8$, $3587 \pm 8$, $3645 \pm 8$, $3740 \pm 8$ yr. These orbits correspond to the finger-like structure of less stable orbits for the case with $I_0 = 0°$.

While the proper frequencies $g$ and $s$ are computed directly with the FMA method, the libration frequency $f_L$ is calculated from the angle $\theta$, the polar angle of the point with Cartesian coordinates $[0.2783 \times (\lambda - \lambda_J - \chi), a - a_J]$ with $\chi = \pi/3$ for $L_4$ and $\chi = 5\pi/3$ for $L_5$ (Milani 1993). The circulation frequency of $\theta$ is computed from the short-term integrations lasting only $2 \times 10^5$. A linear fit to the time series of $\theta$, passed through a digital filter that cuts the frequencies below 15 yr, gives the value of the circulation frequency

of $\theta$ corresponding to the libration period of the critical argument $\lambda - \lambda_J$.

### 3.2 The Lyapunov exponent method

To calculate the Lyapunov exponents for some selected cases we have used the ORBIT9 integrator described in Milani & Nobili (1988) and available at the site tycho.dm.unipi.it/∼planet/software.html.
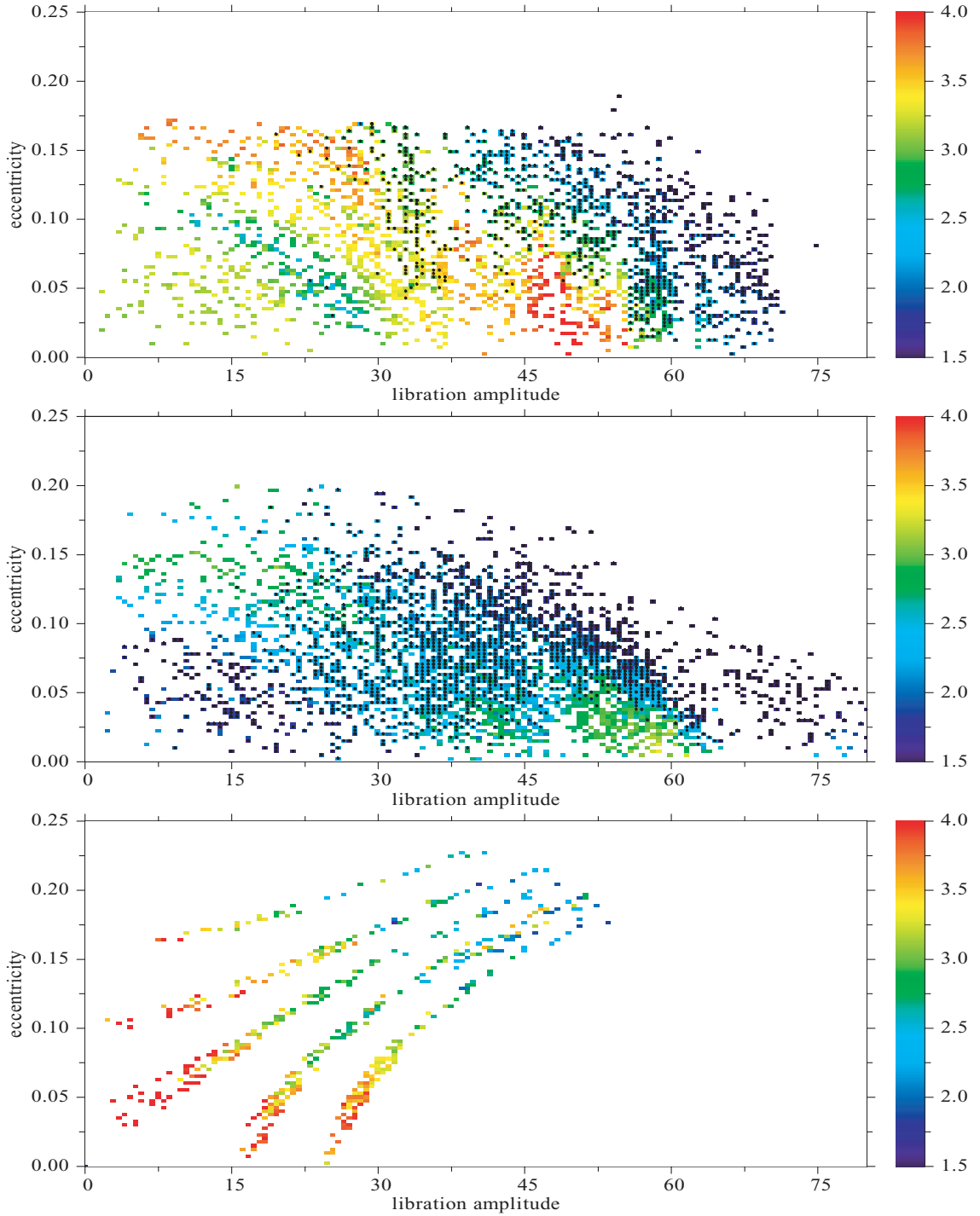
**Figure 3** – *continued*

The numerical code solves both the equation of motion and the corresponding variational equation that is the linearized differential equation of the relative motion between two nearby orbits. An estimate of the maximal Lyapunov characteristic exponent (LCE) that characterizes the rate of exponential divergence between two orbits, is computed as the coefficient of a least-squares linear fit to the function $\gamma(t) = \log[D(t)/D(0)]$, where $D(t)$ is the solution of the variational equation and $D(0)$ is its initial value – a randomly chosen displacement value (Milani & Nobili 1992; Milani 1993).

The variation vector is renormalized when it becomes too large. This method allows one to detect a positive LCE over an integration time-span that is between six and seven times the $1/LCE = T_L$, where $T_L$ is the Lyapunov time. For 75 selected bodies in our sample of virtual Trojans we compute the LCEs with an integration of 100 Myr using a time-step for ORBIT9 of 40 d to avoid the accumulation of rounding-off errors. A value for the slope of $\gamma(t)$ larger than $7 \times 10^{-8}$ is considered as detection of a positive LCE.

## 4 RESULTS

In the colour scale used to represent the local diffusion rate we set an upper limit to the values of $\sigma$. All the orbits with $\sigma \geqslant 4$ have the same colour coding, i.e. red. We set such a threshold because, as shown in Marzari et al. (2002b), it reproduces well the stability area presented by Levison et al. (1997). In other words, the diffusion rate of the orbits coded with red should grant stability at least over the lifetime of the Solar system. We include in each diffusion portrait both $L_4$ and $L_5$ orbits since we did not observe any significant asymmetry, in terms of stability, by comparing separately the diffusion portraits for $L_4$ and $L_5$.

### 4.1 Diffusion portraits

The diffusion portraits of the Trojan orbits for different initial inclination $I_0$ are collected in Fig. 3. As outlined in Section 3, the orbits with $I_p$ out of the band $I_0 \pm 1°$ are marked by a black dot within the coloured data point. In the plot for $I_0 = 0$ the shape of the $s_6$ secular resonances is clearly marked by the dotted data points and the fast diffusion rate may be attributed to this resonance. At higher inclinations, other nodal secular resonances come into play with linear combinations containing the frequencies $s_6$ and $s_7$ (Marzari & Scholl 2002). These resonances introduce peaks that subtract a signal from the proper inclination and, at the same time, contribute to destabilize those orbits with $I_0 \geqslant 20°$ and $s \sim -2 \times 10^{-5}$ to $\sim -4 \times 10^{-5}$. Other orbits with $I_p < I_0 - 1$ are chaotic on their own and the low value of $I_p$ is due to the broadening of the proper peak (see Section 3.1 and Fig. 2). In either case, an orbit with $I_p$ significantly different from $I_0$ is chaotic and the dotted orbits have a fast diffusion rate.

The plots of Fig. 3 show that chaos is also present for non-dotted orbits, while the most stable and compact regions are distributed at low proper values of inclination, libration amplitude, and eccentricity. For $I_0 = 0°$ the stability area reproduces that found by Levison et al. (1997) with an additional small stable area for libration amplitudes between 60° and 75°. In contrast to what Milani (1993) assumed, chaos occurs more often for increasing inclination. At $I_0 = 30°$ the low diffusion area shrinks to a small stripe for libration amplitudes between 45° and 50°. For $I_0 \sim 40°$ all orbits present a high diffusion rate that is characteristic for chaos. The critical question is whether this chaotic behaviour leads the Trojan orbit into an escape route over the lifetime of the Solar system. The FMA method and the Lyapunov exponent computation measure the speed of the chaotic diffusion but cannot predict the size and shape of the stochastic region and, hence, the time-scale for the escape out of the Trojan region. As argued by Milani (1994), orbits with a high diffusion rate in the Trojan regions could be an example of stable chaos, in the sense that the orbits are chaotic but the time-scale for escape is long compared with the diffusion rate. In our previous paper (Marzari et al. 2002b), we integrated the orbits of some high inclined real Trojans that had a high diffusion rate in the proper frequency $g$. All of their trajectories showed large chaotic variations in the libration amplitude but only one was ejected out of the Trojan swarms after 3.5 Gyr (asteroid 12929 TZ1). All the others survived for over 4.5 Gyr. As for other Jovian resonances, this behaviour might be an example of stable chaos where the orbit is 'sticky' to a lower-dimensional torus (Tsiganis, Varvoglis & Hadjidemetriou 2002a,b). To test this possibility we computed the autocorrelation time $\tau_c(L)$ and $\tau_c(G)$ for the Delaunay 'actions' $L = \sqrt{a}$ and $G = \sqrt{a(1-e^2)}$ of all those orbits for which we also computed the LCE (about 30 cases). Apart from a non-significant minority of cases, we did not find the characteristic behaviour of 'sticky' chaos as described in Tsiganis et al. (2002a,b) with $\tau_c(G) \gg \tau_c(L)$, where $\tau_c(L) \sim \tau_{LCE}$. This seems to indicate that the stable chaos of Trojans is not consistent with the 'stickness' hypothesis.

A closer look at the plot for $I_0 = 0°$ reveals several 'finger-like' fine structures of higher diffusion rate within the stable 'red' region. They correspond to very precise frequencies of the perihelion longitude $\tilde{\omega}_T$ of the Trojan orbit for different values of $e_p$ and $D$. Fig. 3 shows a detailed view of these features obtained by selecting bodies with a circulation period $\tilde{\omega}$ equal to 3465, 3527, 3587, 3645 and 3740 yr with a tolerance of $\pm 8$ yr. There are two possible sources of the faster diffusion within these narrow structures: secondary resonances or three-body resonances. Secondary resonances (Lemaitre & Henrard 1990) are commensurabilities between the libration frequency of the critical argument $f_L$ and the circulation frequency of either the argument of perihelion $\omega_T$ or the difference between the perihelion longitude of the asteroid and the planet $\tilde{\omega}_T - \tilde{\omega}_J$. For Jupiter Trojans this interpretation seems unlikely as the libration frequency $f_L$ of the critical argument is significantly faster than the circulation frequency of both the perihelion argument and the longitude. Moreover, it is not possible to reproduce the multiplet structure observed in Fig. 3 with the values of $g$ and $f$ of the Trojan orbits.

Three-body mean motion resonances (Nesvorný & Morbidelli 1999) are probably the best interpretation of the narrow unstable structures. By definition, three-body resonances are described by the relation $m_J\dot{\lambda}_J + m_S\dot{\lambda}_S + m_T\dot{\lambda}_T \sim 0$, where $\lambda_J$, $\lambda_S$ and $\lambda_T$ are the mean longitudes of Jupiter, Saturn and the Trojan, respectively. The mean motions of Jupiter and Saturn are close to a 5:2 resonance, the great inequality. Therefore, we expect that a mixed mean motion resonance of the type $1\dot{\lambda}_J - 5\dot{\lambda}_S + 1\dot{\lambda}_T \sim 0$ may indeed be found within the Trojan orbits since the mean motion of a Trojan orbit is close to that of Jupiter. The critical angles associated with this resonance are any combination of the form $\psi = 1\lambda_J - 5\lambda_S + 1\lambda_T + p_J\tilde{\omega}_J + p_S\tilde{\omega} + p_T\tilde{\omega}_T$, with $p_J + p_S + p_T = k = 3$ to satisfy the d'Alembert rules. The multiplet structure we observe in the $e_P-D$ plane occurs at precise frequencies of $\tilde{\omega}_T$ and, consequently, the splitting in this case is related to different combinations of the perihelia, i.e. different values of the integers $p_J$, $p_S$ and $p_T$. By playing with the frequencies of the orbits located within the 'finger-like' structure, we find that the two combinations 3, $-2$, $-4$ and 4, $-3$, $-4$ may be related to the two main patterns in Fig. 3. Nesvorný & Dones (2002) proposed a different combination of angles, $-7\dot{\lambda}_J + 4\dot{\lambda}_S + 5\dot{\lambda}_T + p_J\tilde{\omega}_J + p_S\tilde{\omega} + p_T\tilde{\omega}_T$ with $p_J + p_S + p_T = k = -2$. We inspected the critical angles of the $k = 3$ and $-2$ three-body resonances, respectively. We found that the $k = 3$ resonances have a circulation period around 5000 yr, while that of $k = -2$ is faster. The multiplet structure then appears to be related to the $k = 3$ resonances. At higher inclinations, the multiplet structure disappears as the frequency of $\tilde{\omega}$ moves to lower values. A trace of this structure may be seen at libration amplitudes between 30° and 45° in the plot of $I_0 = 10°$.

In the two plots at inclinations $I_0 = 0°$ and 10° a large V-shaped chaotic zone cuts through the compact stable red region. This chaos is not related to a single frequency of the perihelion longitude circulation or of the critical libration argument. It is integrated over a range of frequencies of these two angular variables. The V-shaped zone in fact covers a large range in $D$ and, consequently, a wide range in both $g$ and $f$. It cannot entirely be attributed to nodal secular resonances, even if at 10° most of the bodies within the V-shaped structure are marked by a dot and at $I_0 = 0°$ the $s_6$ secular resonance is clearly visible at the border of the unstable region. In fact,

in many cases the low value of $I_p$ can be due to the broadening of the peak in $p$, $q$ generated by the chaotic wandering of the frequency $s$: the chaos is not necessarily caused by a nearby secular resonance.

By inspecting the results of the three-body integration (see Section 4.3), a trace of this structure appears when Jupiter is on a highly eccentric orbit. However, additional perturbing terms must come into play in the full six-body model to justify the extent of the V-shaped unstable area. Marzari & Scholl (2002) showed that perturbations by Saturn not related to low-order resonant frequencies can indeed destabilize Jupiter Trojans. Why non-resonant? Because similar escaping rates were found even when Saturn was shifted from its present orbit further away from the 5:2 resonance with Jupiter within a 'static' four-body model with Jupiter and Saturn on fixed elliptical orbits. Three-body mean motion resonances also contribute to the chaotic evolution, as suggested by Nesvorný & Dones (2002). The multiplet structure at $I_0 = 0°$ is strong evidence for their involvement. At higher inclinations, nodal secular resonances begin to grow in strength and they possibly explain the enlargement of the chaotic zone until, at $I_0 = 40°$, no stable orbits are found.

## 4.2 Comparison between the FMA and the Lyapunov exponent method

A common feature of the FMA method and of the computation of the maximal LCE is that they both measure the rate at which a chaotic orbit separates from its initial position in the action space. We then expect that the two indicators of diffusion rate, the value of $\sigma$ for the FMA method and the estimated maximal LCE $\chi$, are in agreement. We selected 75 virtual Trojan orbits from our sample and computed both $\sigma$ and $\chi$ for each. Out of these, 25 are coded red with the FMA method, i.e. they have a slow diffusion rate ($\sigma > 4.0$) and are possibly stable on a long time-scale. They are randomly chosen within the stability regions shown in Fig. 3 and they belong to different slices in inclination. Another 25 are coded green ($2.8 < \sigma < 3.2$) and have a faster diffusion rate. The remaining 25 are coded blue ($\sigma < 2.0$) and are highly chaotic according to the FMA method.

In Fig. 4 we show a histogram of the maximal LCEs for the same 75 orbits using a different shadowing according to the colour
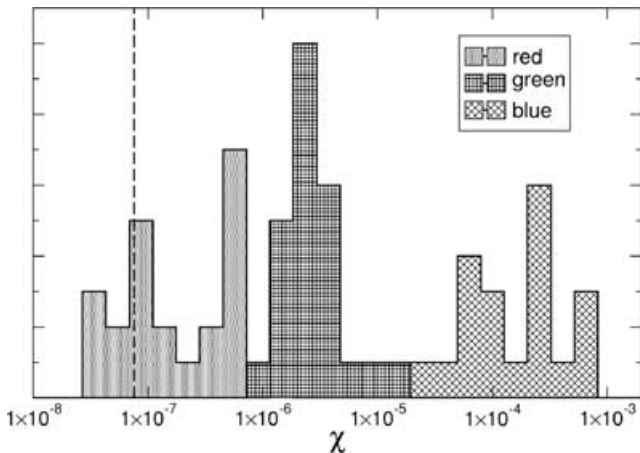


**Figure 4.** Histogram showing the number of virtual Trojans with a given value of maximal LCE. The three groups characterized by different values of $\sigma$ computed with the FMA method, are also well separated in terms of maximal LCE value. The dashed vertical line is the minimum value of $\chi$ required for positive detection of chaos in our integrations lasting 100 Myr.

coding of $\sigma$. We notice that the orbits with smaller values of $\sigma$ are also those with a lower value of $\chi$. The green coding of the FMA method shows larger values of $\chi$, and the blue orbits have Lyapunov times $T_L$ smaller than $1 \times 10^4$ yr. The two indicators of diffusion rate are in very good agreement and we can associate to the red areas of Fig. 3, where the real Trojans are located, maximal Lyapunov exponents smaller than $1 \times 10^{-6}$.
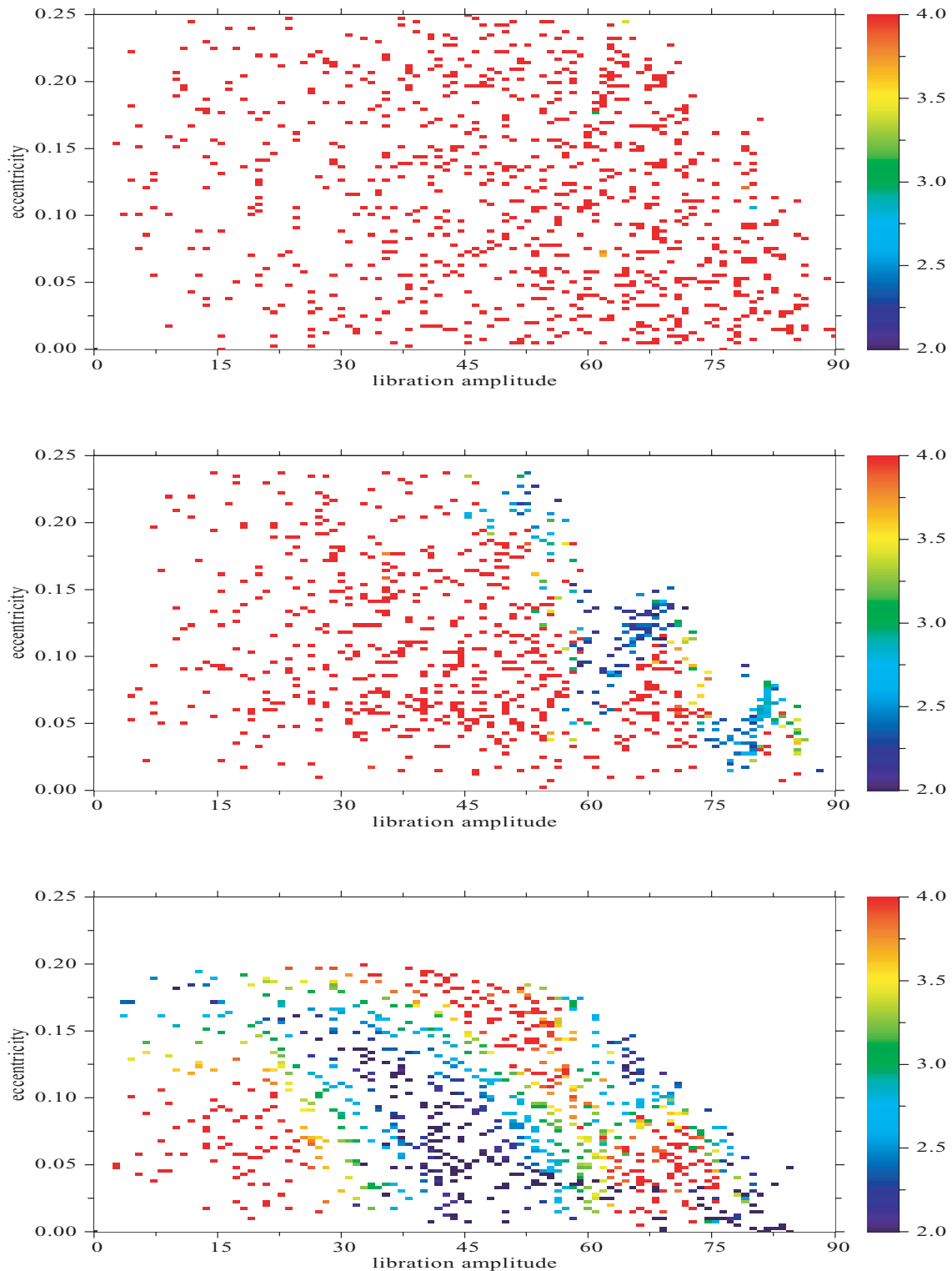
## 4.3 The three-body model

In order to test to what extent the stability of Jupiter Trojans is due to the presence of the outer planets, we integrated the orbits of Jupiter Trojans within three three-body models with a fixed eccentricity of Jupiter equal to 0, 0.048 (the mean value) and 0.065 (the maximum value), respectively. In addition, we considered two different initial inclinations for the Trojans: 0° and 40°. The outcomes in term of diffusion rates are shown in Fig. 5. The diffusion rates are coded as in Fig. 3 and all orbits with $\sigma$ greater than 4, and possibly stable over a long time-scale, are red. However, by comparing the values of $\sigma$ for Trojan orbits in the six-body model and in the three-body model, we noticed that in many cases in the three-body case the value of $\sigma$ was significantly larger, even 6 or 7, indicating a higher orbital stability. The perturbations by the outer planets increase the diffusion rate even in the more stable regions.

As in the six-body case, also in the three-body case, the stability region is limited in the $D$–$e_p$ plane, which is possibly due to the complete overlap of resonances of first order in eccentricity that sequentially accumulate to create a stochastic region around the orbit of the planet (Wisdom 1980). The Lagrangian points of Jupiter are embedded in this stochastic layer that grinds the outer edge of the Trojan stability region. For the higher eccentricity of Jupiter the chaos is stronger around the orbit of the planet and this further narrows the stable area around $L_4$ and $L_5$. In particular, in the case with $I_0 = 0°$, a fast diffusion region begins to pierce the stable area for libration amplitudes around $D \sim 60°$. In Fig. 5 we notice that the case with $e_J = 0.065$ begins to show the above quoted V-shape unstable area that is not present in the case with $e_J = 0$. The same V-shape structure is present in the case with $e_J = 0.048$ but it is slightly less extended. For highly inclined orbits ($I_0 = 40°$) the stability is strongly affected by the eccentricity of Jupiter. If $e_J = 0$ the stable region is only slightly smaller than the corresponding case with $I_0 = 0°$ and $e_J = 0$. When the eccentricity of Jupiter is set equal to $e_J = 0.048$ the stable region is crossed by stripes of fast diffusion and the area where stable orbits are located is strongly reduced.

The existence of stable high-inclination orbits in the three-body model suggests that the corresponding lack of stable orbits in the six-body case is possibly due to the perturbations of the outer planets, in the form of secular resonances or three-body resonances.

## 5 A SEMI-ANALYTICAL MODEL FOR SECULAR BEHAVIOUR

The FMA analysis has provided us with a list of the proper elements and the corresponding proper frequencies for a large number of Trojan orbits. An immediate step is to perform a numerical fit to the proper frequencies with a polynomial expression to build up a semi-empirical secular theory for the Trojan motion. This study was already performed by Schubart & Bien (1987) with 40 Trojan orbits, and it was subsequently improved by Milani (1994) who used a sample of 174 real Trojans. We have adopted the same polynomial form of Milani and we have tested the fitting algorithm on a

**Figure 5.** Diffusion portraits of Trojans orbits integrated within the three-body model. From top to bottom: $I_0 = 0°$ and $e_J = 0$, $I_0 = 0°$ and $e_J = 0.065$, and $I_0 = 40°$ and $e_J = 0.048$.

sample of real Trojan orbits similar to that used by Milani. The co-efficients of the polynomial expressions we found were very similar to those obtained by Milani giving reliability to the procedure. We then analysed about 10 000 Trojan orbits well sampled in the proper elements space $D$, $e_p$ and $I_p$, also covering regions of the action

space where real Trojans are not found. In the sample of orbits to be fitted we include only those bodies that are within the previously defined bands in inclination ($I_0 - 1° < I_p < I_0 + 1°$). In this way we neglect orbits not having well-defined values of $I_p$ or having the frequency $s$ changing chaotically on a short time-span. The analytical

expression adopted by Milani (1994) has been used and our best fit is

$$s = -8.56 - 8.07x^2 + 17.39y^2 - 28.72z^2 - 0.42x^2y^2$$
$$- 2.46y^4 + 3.83x^4 + 4.69y^2z^2 + 6.60z^4$$

$$g = 364.81 - 13.60x^2 - 138.30y^2 + 61.52z^2 + 2.31x^2y^2$$
$$+ 10.75y^4 - 13.52x^2z^2 - 78.99y^2z^2 - 7.18z^4$$

$$f_L = 8856.60 + 76.26x^2 - 2045.31y^2 - 675.50z^2 - 239.54x^2y^2$$
$$+ 951.75y^4 - 33.40x^2z^2 + 43.75y^2z^2 + 42.16z^4$$

with

$$x = \frac{e_p}{0.15} \qquad y = \frac{\sin I_p}{0.6} \qquad z = \frac{da}{0.15\,au}. \qquad (3)$$
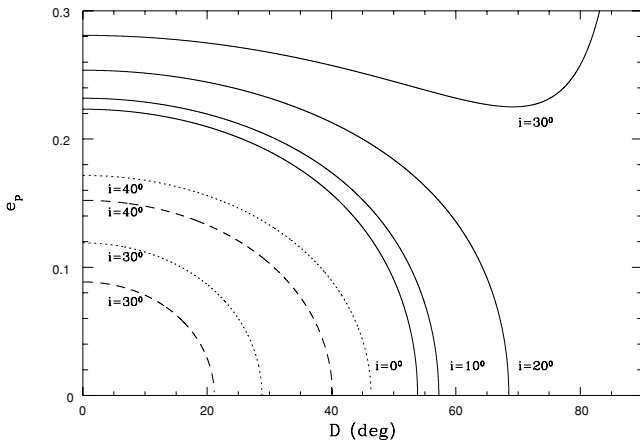
The relative error in each coefficient was less than 1 per cent. The frequencies $g$, $s$ and $f_L$ are expressed in arcsec yr$^{-1}$. We do not compute $da$ directly from our numerical integration, but rather $D$. However, to compare with Milani's best fits we transform $D$ to $da$ using the formula $D = da/0.2783$ (Erdi 1988; Milani 1993). The coefficients are of the same order of magnitude but significantly different from those of Milani (1994), possibly because the real Trojans cover only a limited region of the phase space. Moreover, our sample is about 50 times more populated than that used by Milani.

Given the proper frequencies, in particular $s$, we can identify the main secular resonances within the Trojan regions. In Fig. 6 we plot in the space $D$–$e_p$ the major secular resonances for different inclinations, $s_6$, $s_7$ and $s_8$. In Fig. 7 we concentrate on the case with $I_0 = 40°$ and we outline possible secular resonances that can explain the high diffusion rate of the high inclined Trojan orbits.
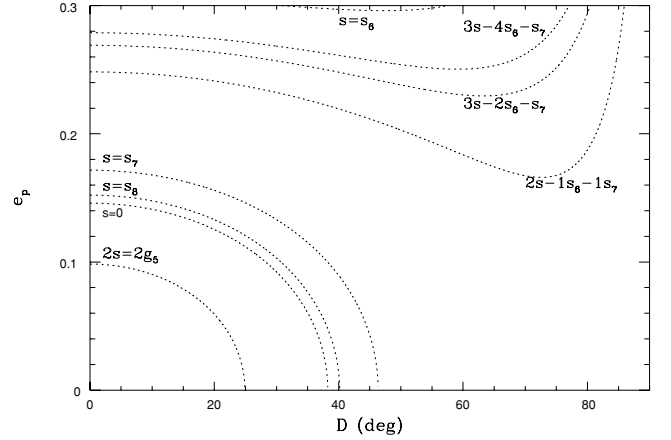
## 6 DISCUSSION

The FMA method is a powerful tool for measuring the diffusion rate of orbits in the action space and it can be successfully used for outlining the regions where stable or chaotic orbits can be found. We have applied the FMA to Trojan-type orbits of Jupiter to detect where primordial bodies may have survived from the origin of the Solar system until the present. The stable regions are characterized by low diffusion rates and stability is granted over 4.5 Gyr. At low inclination the stablity we outline with the FMA method matches that found by Levison et al. (1997) by direct numerical integration.

It remains an open question for Jupiter Trojans, and maybe for Trojans in general, whether a fast diffusion rate, and then chaos,
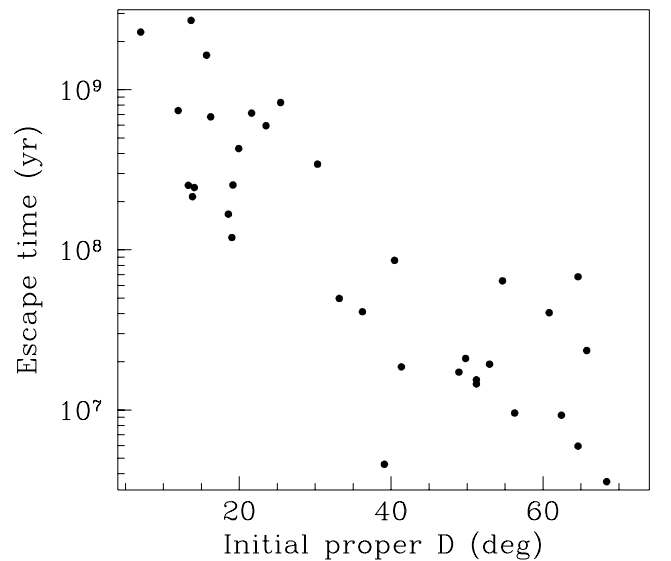
**Figure 7.** Secular resonances location in the $D$–$e_p$ plane for $I_0 = 40°$.

always implies a quick escape from a Trojan orbit. Milani (1993, 1994) argued that some Trojan orbits may be examples of stable chaos: their evolution is chaotic but the size of the stochastic layer may be limited or, perhaps, its structure may be very complex. This seems to be the case for some high-inclination Trojans. According to the FMA method all orbits with an inclination of $I_0 = 40°$ are chaotic with a fast diffusion rate but, at present, we know some real Trojans (three numbered and two unnumbered) with inclinations around 40°. They may not be primordial and may be the results of recent collisional events that ejected them into their present orbits. However, the orbits of three of these bodies have been numerically integrated by Marzari et al. (2002b) for 4.5 Gyr and two of them survive, even showing strong chaotic variations of the libration amplitude and eccentricity. Their diffusion rate is similar to that of low-inclination and large libration amplitude (or high-eccentricity) Trojan orbits which, on the other hand, escape on time-scales of the order of $10^7$–$10^8$ yr.

Marzari et al. (2002b) identified different routes that take a Trojan out of the resonant region: the libration amplitude $D$ grows,

**Figure 6.** Major secular resonances in the $D$–$e_p$ plane. The continuous line marks the location of the $s_6$ resonance for different inclinations, the dashed line the location of the $s_7$, and the dotted line that of the $s_8$.
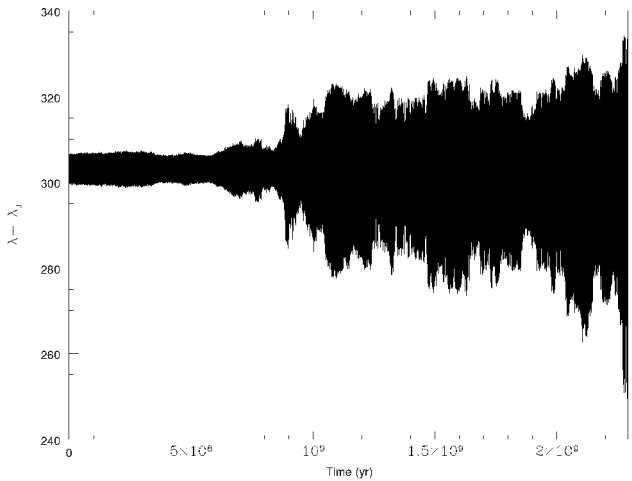
**Figure 8.** Survival times for bodies with $I_0 = 40°$, proper eccentricity $e_p < 0.1$, $\sigma \sim 2$ and $D_0$ distributed between 0° and 70°. Bodies initially having a lower value of $D_0$ survive longer.

**Figure 9.** Chaotic evolution with time of the libration amplitude $D$ for a body with $I_0 = 40°$, $e_p < 0.1$ and $\sigma \sim 2$. The escape from the Trojan orbit occurs at $t = 2.3$ Gyr after a close encounter with Jupiter.

while on average the proper eccentricity is constant, until the asteroid encounters the planet and is ejected out of the resonance, or the eccentricity increases, while $D$ is constant, and again a close encounter pushes the asteroid out of the libration region. There is a simple interpretation that allows one to comply with the FMA predictions that highly inclined Trojan orbits are unstable while real Trojans such as (29976) 1999 NE9 and (24449) 2000 QL63 survive over 4.5 Gyr. In spite of their high diffusion rate, these two bodies start on a low libration amplitude and low-eccentricity orbit. It would take them more time to cover the chaotic route that leads to high values of eccentricity and libration amplitude and then to a close encounter with Jupiter.

In order to test this hypothesis we integrated 35 of our virtual Trojans over a long time-span. The bodies are selected among those with inclination $I_0 = 40°$ with the following properties: a fast diffusion rate $\sigma \sim 2$, proper eccentricity lower than 0.1, libration amplitude evenly distributed between $0°$ and $70°$. In Fig. 8 we show the time survived by each test body as a function of the initial proper libration amplitude $D_0$. The linear trend (in logarithmic scale) seems to confirm that bodies with lower $D_0$ take more time to escape notwithstanding the fact that they have the same diffusion rate. The scattering of the data may be enhanced by the fact that the bodies do not have initially exactly the same proper eccentricity. Moreover, we expect that the chaotic route to escape is a random walk, as illustrated in Fig. 9, an example of a high-inclination chaotic orbit.

The location of the libration centre is displaced for the equilateral configuration due to the high inclination of the orbit. This behaviour is described in detail in Namouni & Murray (2000) and Nesvorný et al. (2002).

In conclusion, the FMA method works well to determine the chaotic nature of Trojan orbits. However, the relationship between the diffusion rate and the escape time must be handled with care due to the complexity of the Trojan motion.

## REFERENCES

Beaugé C., Roig F., 2001, Icarus, 153, 391
Carpino M., Milani A., Nobili A.M., 1987, A&A, 181, 182
Erdi B., 1988, Cel. Mech., 43, 303
Laskar J., 1993a, Physica D, 67, 257
Laskar J., 1993b, Cel., Mech. Dyn. Astron., 56, 191
Laskar J., Froeschlè C., Celletti A., 1992, Physica D, 56, 253
Lemaitre A., Henrard J., 1990, Icarus, 83, 391
Levison H., Duncan M.J., 1994, Icarus, 108, 18
Levison H., Shoemaker E.M., Shoemaker C.S., 1997, Nat, 385, 42
Marzari F., Scholl H., 2002, Icarus, 159, 328
Marzari F., Tricarico P., Scholl H., Michel P., 2002a, AAS DPS meeting 34, abstract no. 02.07
Marzari F., Tricarico P., Scholl H., 2002b, ApJ, 579, 905
Marzari F., Scholl H., Murray C., Lagerkvist C.-I., 2003, in Bottke W., Cellino A., Paolicchi P., Binzel R.P., eds, Asteroids III. Univ. Arizona Press, Tucson, p. 725
Milani A., 1993, Cel. Mech. Dyn. Astron., 57, 59
Milani A., 1994, ACM 1993, p. 159
Milani A., Nobili A., 1988, Cel. Mech. Dyn. Astron., 43, 1
Milani A., Nobili A., 1992, Nat, 357, 569
Namouni F., Murray C.D., 2000, Cel. Mech. Dyn. Astron., 76, 131
Nekhoroshev N.N., 1977, Russ. Math. Surveys, 32, 1
Nesvorný D., Dones L., 2002, Icarus, 160, 271
Nesvorný D., Morbidelli A., 1999, Cel. Mech. Dyn. Astron., 71, 243
Nesvorný D., Thomas F., Ferraz–Mello S., Morbidelli A., 2002, Cel. Mech. Dyn. Astron., 82, 323
Šidlichovský M., Nesvorný D., 1997, Cel. Mech. Dyn. Astron., 65, 137
Schubart J., Bien R., 1987, A&A, 175, 299
Tsiganis K., Varvoglis H., Hadjidemetriou J.D., 2002a, Icarus, 155, 454
Tsiganis K., Varvoglis H., Hadjidemetriou J.D., 2002b, Icarus, 159, 284
Wisdom J., 1980, AJ, 85, 1122
Wisdom J., Holman M., 1991, AJ, 102, 1528

This paper has been typeset from a TEX/LATEX file prepared by the author.